Density resolution in quantitative computed tomography of foam and lung

Gerrit J. Kemerink, Han H. Kruize, Rob J. S. Lamers,
and Jos M. A. van Engelshoven
Department of Radiology, University Hospital Maastricht, P. Debyelaan 25, PO Box 5800, 6202 AZ Maastricht, The Netherlands

(Received 23 February 1996; accepted for publication 21 July 1996)

This study was performed to assess density resolution in quantitative computed tomography (CT) of foam and lung. Density resolution, a measure for the ability to discriminate materials of different density in a CT number histogram, is normally determined by quantum noise. In a cellular solid, variations in mass in the volumes sampled by CT cause an additional degradation of density resolution by the linear partial volume effect. The sample volume, which is directly related to spatial resolution, can be varied by choosing different section thicknesses and reconstruction filters. Several polyethene (PE) foams, as simple models of lung tissue, and five patients were investigated using various sample volumes. For the uniform PE foams, density resolution could be directly determined as the full width at half maximum of CT number histograms. Density resolution for foams with cell sizes of 0.8–1.5 mm was dominated by effects caused by the limited sample size, not by quantum noise. The relative magnitudes of density resolution could roughly be explained with a model for a hypothetic random cellular solid. Since lungs are not of uniform density, analysis of patient data was more complicated. A combined convolution least-squares fit procedure, together with information obtained in the studies of foam, were used to determine density resolution in lung studies. Density resolution, both for foams and lung, was strongly dependent on sample volume, and was quite poor for thin sections and sharp filters. Consequently, histogram-shape related parameters are sensitive to the spatial resolution chosen on CT. Thin section densitometry, using a 1-mm section with a standard or high resolution filter, is not recommended except in determining average density. When using thicker sections, an in-plane spatial resolution similar to section thickness is advised.

Key words: densitometry, lung density, CT technology

I. INTRODUCTION

Modern computed tomography (CT) scanners are able to determine the average density of lung tissue with acceptable accuracy.[1,2] With proper air calibration the average lung density, as determined by CT, is largely independent of the scanner's technique settings, and results from different scanners can meaningfully be compared, at least for a number of widely used scanners that was recently tested.[2]

However, disease affecting lung density only locally, or to varying degrees throughout the lung, may not optimally be reflected by the average density. Such lesions might in principle be quantified more effectively using other quantities derived from CT number histograms. Several investigators, following this approach, have tried to quantify the extent and severity of emphysema and interstitial lung disease. They used, among others, the fractional area of the histogram below some threshold (also referred to in the literature as pixel index or density mask),[3–12] a percentile (being the CT number below which a given percentage of the histogram extends),[5,12–17] the fraction of the histogram within a given interval or above some CT number,[16–20] the standard deviation and full width at half maximum (FWHM),[14,15,18] and the skewness and kurtosis.[21] Unfortunately, these parameters are dependent on all instrumental factors that affect the shape of the histogram. Among these instrumental factors section thickness and reconstruction filter (or kernel) are of paramount importance. According to the literature cited, section thicknesses from 1 to 13 mm have been used, while only standard and high resolution reconstruction filters have been applied. Although all investigators who performed histogram analysis appeared to be aware of the dependence of the CT number distribution on scanning technique and reconstruction kernel, no quantitative study of the effect of these parameters has been published to our knowledge. This is a very unsatisfactory state of affairs since it is by no means obvious that the techniques described in the literature are well suited to their purpose.

In order to facilitate a quantitative description of factors affecting parameters derived from a histogram, it is practical to introduce the quantity "density resolution." Density resolution, for a certain material and a given set of CT technique parameters, is defined as the FWHM of the CT number histogram of a large sample of uniform density of that material. To conform with definitions of resolution in other fields of spectroscopy, the FWHM was chosen as the descriptive parameter rather than the standard deviation. For water equivalent tissue, like the lung,[22] density resolution has numerically the same value when expressed in Hounsfield units (H) or kg/m^3. The importance of density resolution may immediately be evident from the fact that it is the lower limit by which two tissues (e.g., healthy and diseased lung) have

 0094-2405/96/23(10)/1697/12/$10.00

to differ in density in order to be seen separately in a CT number histogram. A quantity related to density resolution, but distinctly different and unfortunately of little use in the present context, is the generally used (low) contrast resolution, defined as the diameter of a circular region that, at a given difference in CT number, makes the region just discernible from its surroundings.[23] This parameter is generally specified in CT product data.

For a noncellular material of uniform density, like water or air, density resolution in CT is normally limited by quantum noise, i.e., by the finite number of photons that is detected after transmission of the x rays through the phantom. A cellular material, like foam or lung, further degrades density resolution by the linear partial volume effect. The underlying physical mechanism is that, in sampling an air containing cellular solid, the individual samples will contain varying amounts of air and solid. The degree of deterioration of density resolution is strongly dependent on the ratio of the spatial resolution chosen on the CT system, and the characteristic dimensions of the cellular structure. For clinical applications the spatial resolution should ideally guarantee the sampling of areas affected by disease without the inclusion of unaffected tissue, while at the same time the density resolution should allow discrimination between affected and unaffected tissue.

The aim of the present study was to provide quantitative data on the relation between spatial and density resolution. This information should be of help in choosing an optimal compromise between the conflicting demands for both kinds of resolution. To this purpose the following points were addressed: (1) By way of introduction the effect and importance of density resolution will be illustrated using a phantom containing foams of two densities. (2) Measurements of the in-plane spatial resolution for the CT's various reconstruction filters will be performed. Together with section thickness, this in-plane spatial resolution enables the calculation of the nominal sample volume of the CT scanner. (3) Density resolution for polyethene (PE) foam, as a simple model for lung tissue, will be studied in some detail. (4) The contribution of quantum noise to density resolution will be investigated. (5) Density resolution in patient studies of lung will be estimated.

II. MATERIALS AND METHODS

A. Phantoms and patients

A thin copper wire (0.15 mm in diameter) was used as a resolution phantom to determine the point spread function (PSF) for the CT's various reconstruction filters.

Polyethene (PE) foam samples of several densities (37, 59, 63, 96, 109, 164, and 186 kg/m^3; PSG, Wellen, Belgium) have been used as pseudo-lungs. We will refer to these foams by means of their density. These samples were studied free in air on the patient bed, in the empty lower section of a humanoid thorax phantom,[24] and in a polymethylmethacrylate (PMMA or perspex) phantom. The PMMA phantom has the form of a cross-sectional slice of an average human thorax, with cavities in the positions of the lungs. Air, in the empty cavities of the phantoms, was also measured to estimate system noise.

In this study five male patients were included: three patients with emphysema (A: 68 y; B: 63 y; C: 79 y), one patient with normal lungs (D: 69 y), and one patient with both emphysema and interstitial lung disease (E: 83 y). Our lung density research protocol was approved by the Medical Ethical Committee of our institution, and the studies were performed after obtaining the patient's informed consent.

B. CT scanner

All measurements were performed on a Somatom Plus scanner (Siemens, Erlangen, Germany). The high voltage was in all cases 137 kV. Unless stated otherwise, we used a scanning time of 1 s, a tube load of 220 mAs, a zoom factor in reconstruction of 1.6, and a 512×512 matrix. At 220 mAs the system used the large focal spot of the x-ray source. Reconstruction kernels (or filters) applied in this study were: ultra-high resolution (UHR; Siemens code AB_07041), high resolution (HR; AB_07052), standard (STD; AB_07055), soft (SFT; AB_07057), and detail soft (DS; AB_07059). We will refer to this set as "the five kernels" or "all five kernels."

C. Measurements

To illustrate the effect of density resolution measurements were performed on the PMMA thorax phantom equipped with two PE foams: 75% of the area of one lung cavity was filled with foam of a density of 96 kg/m^3, while the remaining 25% was filled with foam of a density of 63 kg/m^3, simulating a large lesion of lower density. The other lung cavity was left empty (thus air filled) to yield estimates of system noise within an average sized thorax. Section thicknesses of 1, 2, 3, 5, and 10 mm were applied, and each scan was reconstructed with all five kernels mentioned before. The degree of separation of the two foams in the CT number histogram will give a simple visual indication of density resolution.

In order to find the in-plane sample size the thin copper wire (resolution phantom) was imaged with a section thickness of 3 mm and reconstructed with all five kernels using a large zoom factor of 16 (field of view approximately 3 cm).

To find the density resolution for foams, PE foams 37, 59, 109, 164, and 186 have been measured in air (foam free on patient bed) with the same section thicknesses and reconstruction filters as used with the PMMA phantom. For a few acquisitions the images were reconstructed with zoom factors other than 1.6 to check the effect of this parameter.

To verify the uniformity of the foams, larger CT sample volumes are required than achievable with the DS kernel. Therefore, the matrix size of the image was reduced from the original 512×512 to 64×64 by taking the average of sets of 8×8 pixels. We used 10-mm sections and the STD filter in this last experiment.

The effect of quantum noise was investigated using foam 37 and air within the humanoid thorax cavity. The phantom

was surrounded by an additional ring of fat of 3 cm thickness. This foam and the "obese" phantom were chosen because they realized similar contributions of quantum noise and sampling effects to density resolution. Technique settings were: a section thickness of 1 mm, the STD reconstruction kernel, and various tube loads between 75 and 880 mAs, with corresponding scan times between 1 and 4 s.

All five patients were investigated at only one anatomical position, at full inspiration, and using section thicknesses of 1, 2, 3, 5, and 10 mm. Each scan was reconstructed with all five kernels, resulting in 25 images per patient.

D. Theory of analysis

The definition of density resolution, as given in Sec. I, has the following background: Consider a cellular material of uniform average density that is scanned using sample volumes of such a large size that the resulting CT number histogram has a negligible width. Choosing smaller sample volumes causes an increase in the relative variation in mass sampled. By the linear partial volume effect this is reflected in an increase in spread in CT numbers in the image, thus in a broadening of the histogram. Since nonlinear effects are very small,[25] the average CT number will remain the same. Except for normalization, the measured, broadened histogram can be seen as the convolution function applied to the original spikelike histogram. The function's width is then, by common definition, the resolution. Thus, provided that the foams used are of uniform average density, and we will show they are, the measured histograms yield a direct estimate of density resolution. We will see that for the foams the measured histograms resemble Gaussians, except for some tailing toward higher CT numbers. To quantify this tailing the skewness of the histogram was also determined.

For lung tissue the situation is more complicated. Because lung tissue is not of uniform average density, the FWHM of the CT number histogram of a patient does not reflect density resolution in a direct way. But even for arbitrary density distributions in the lung, it should be possible to find the difference in density resolution between two different measurements using convolution techniques. We tried to realize this in the following way. We took the reconstruction with the detail soft kernel (DS; AB_07059) as the reference, and assumed that at the corresponding scale of sampling the average density within each sample might still be considered constant. Histograms obtained using sharper kernels should be obtainable from the DS histogram by convolution with a suitable function, the width of the convolution function reflecting the difference in density resolution between the two kernels. To keep the analysis tractable we assumed that the convolution functions could be approximated with Gaussians. The analysis was performed per series of one section thickness, because different sections contain different tissue and are for that reason difficult to compare.

One expects the width of the convolution function to be dependent on the local density ρ and the characteristic size D of the cellular lung structure. Not having any knowledge on the local D we tried to model the sampling component of density resolution for lung tissue as

$$\mathrm{FWHM}(S,F,\rho)=\mathrm{FWHM}(S,F).(\rho/\rho_{\mathrm{av}})^{\gamma}, \tag{1}$$

with S the section thickness, F the reconstruction filter, ρ (ρ_{av}) the (average) lung density, and γ some positive power. This ρ dependence assures that the width of the convolution function becomes zero when density does. For a truly random solid with a fixed D one expects $\gamma=1$ (see hereafter). Introduction of the power γ creates an additional degree of freedom. In this model the width of the convolution Gaussian, required to convert the reference DS histogram into one corresponding to filter F, is given by

$$\mathrm{FWHM}(S,\mathrm{DS}\rightarrow F,\rho)=\mathrm{FWHM}(S,\mathrm{DS}\rightarrow F).(\rho/\rho_{\mathrm{av}})^{\gamma}, \tag{2}$$

with $\mathrm{FWHM}(S,\mathrm{DS}\rightarrow F)$

$$=\sqrt{\mathrm{FWHM}^2(S,F)-\mathrm{FWHM}^2(S,\mathrm{DS})}. \tag{3}$$

Here we used the property that the convolution of two Gaussians is again a Gaussian with a width given by a formula well known from error propagation analysis. In the presence of quantum noise, (3) becomes

$$\mathrm{FWHM}(S,\mathrm{DS}\rightarrow F,QN,\rho)=\sqrt{\mathrm{FWHM}^2(S,\mathrm{DS}\rightarrow F).(\rho/\rho_{\mathrm{av}})^{2\gamma}+\mathrm{FWHM}^2_{QN}(S,F)-\mathrm{FWHM}^2_{QN}(S,\mathrm{DS})}, \tag{4}$$

with $\mathrm{FWHM}_{QN}(S,F)$ the FWHM of the CT number histogram of air acquired under the same conditions of kV, mAs, x-ray attenuation, and scatter as in the patient study.

Estimates of $\mathrm{FWHM}(S, \mathrm{DS}\rightarrow F)$ were determined from a one parameter fit using (4) in a convolution algorithm that was incorporated in a general nonlinear least-squares fit procedure.[26] Thus, $\mathrm{FWHM}(S, \mathrm{DS}\rightarrow F)$ was determined in such a way that the convolution of the measured DS histogram with a Gaussian of the width given by (4), fitted optimally in the least-squares sense to the measured histogram corresponding to filter F. The parameter γ was determined beforehand by varying its value, performing a number of fit procedures, and evaluating the quality of the fits as reflected by χ^2. The γ so found was used throughout the complete analysis of that patient.

The foregoing procedure yields only differences in density resolution, while we are interested in absolute values. However, calculation of absolute values is possible when a second relation can be found. This relation might be obtained from the PE foam studies. There it was found that the ratio $\alpha_s \equiv \mathrm{FWHM}(S,\mathrm{DS})/\mathrm{FWHM}(S,\mathrm{SFT})$ was nearly independent of foam type. Assuming that the ratio is the same for lung,

one can convert the relative FWHMs into absolute values. First we calculate FWHM(S,DS) using α_s:

$$\mathrm{FWHM}(S,\mathrm{DS}) = \mathrm{FWHM}(S,\mathrm{DS}\rightarrow\mathrm{SFT}).\ \frac{\alpha_S}{\sqrt{1-\alpha_S^2}}, \tag{5}$$

then all other FWHM(S,F) using (5):

$$\mathrm{FWHM}(S,F) = \sqrt{\mathrm{FWHM}^2(S,\mathrm{DS}\rightarrow F) + \mathrm{FWHM}^2(S,\mathrm{DS})}, \tag{6}$$

for F=SFT, STD, HR, or UHR, so that in the presence of quantum noise

$$\mathrm{FWHM}(S,F,QN,\rho) = \sqrt{\mathrm{FWHM}^2(S,F).(\rho/\rho_{\mathrm{av}})^{2\gamma} + \mathrm{FWHM}^2_{QN}(S,F)}, \tag{7}$$

with FWHM(S,F) according to (5) or (6).

E. Practical analysis

All reconstructed CT images were transferred to an ICON Power PC workstation (Siemens Gammasonics, Hoffman Estates, IL) for further processing with software developed in our hospital.

CT images of foam in air, and air itself, were analyzed using the same elliptical region of interest (ROI) on all images of a series. The area of the ROI was always as large as possible, typically 110 cm^2. CT number histograms were generated from the part of the images within the ROI. The following parameters were determined from the histograms: the FWHM, the average CT number, the standard deviation, and the skewness. A series consisted of 25 images (five section thicknesses, five kernels). It turned out that the directly measured FWHM was prone to statistical variations in the histogram. Since the standard deviation (s.d.) was far more robust, we calculated for each foam the average ratio of FWHM and s.d., and used this ratio to calculate an effective FWHM (the density resolution) from the standard deviation.

Only one lung in the images of the patients was analyzed in order to limit the amount of work and data. In a series of 25 images from one patient, the (whole) selected lung was automatically segmented in one image only, and the segmented area slightly eroded so that the resulting region fitted also within the lung in all other images, even when small differences in "full" inspiration were present. This procedure was followed to ascertain that all histograms were from the same area of lung, containing the same number of pixels. Quantitative analysis was performed per series of five images of the same section thickness, the images in a series differing only in the reconstruction kernel that had been applied. The results obtained by fitting expression (4) were converted to absolute estimates of density resolution using (5) and (6). Values for quantum noise needed in using (4) were obtained from the air-filled lung cavity of the PMMA phantom.

F. Sampling within a hypothetical random cellular solid

Unfortunately, as far as we know, no model has been published that describes the distribution of mass in samples arbitrary taken out of foam or lung tissue. In order to gain at least some insight into the problem, consider a hypothetic foam of average density ρ, consisting of randomly distributed, but identical structure elements. Structure elements might be seen as idealizations of faces and edges of the polyhedral cells of, for instance, PE foam. For a tetrakaidecahedron, as for PE, there is a fixed average number n (of about 19) of these structure elements per cell volume.[27] Suppose the cell volume is D^3. In a sample volume V there will be on average $N=nV/D^3$ structure elements, with, according to Poisson statistics, a standard deviation (s.d.) of $\sqrt{N}$. Since the average density in the sample volume is ρ, its s.d. is given by s.d.$=\rho\sqrt{N}/N$. Using $V=SL^2$, with S section thickness, and L the effective in plane sample size, one gets

$$\text{s.d.} = \sqrt{\frac{D^3}{nV}}\,\rho = \sqrt{\frac{D^3}{nS}}\,\frac{\rho}{L}. \tag{8}$$

Obviously, this model neglects the order present in cellular solids. For volumes not too small compared to cell size, the model may not be wholly unrealistic since there exists considerable variation in both cell size and cell form in foams. We will refer to this model as the random cellular solid model.

Note that according to this model the s.d. in CT estimated density has the same functional dependence on section thickness and in-plane resolution as the s.d. due to quantum noise.

III. RESULTS

A. Illustration of effect of density resolution

Histograms from the PMMA thorax phantom equipped with PE foams of two different densities are shown in Fig. 1. As an example the image of the PMMA phantom, obtained with a section thickness of 1 mm and the UHR reconstruction filter, is displayed in Fig. 2. The histogram in the left top of Fig. 1 corresponds to this image.

B. Spatial resolution

The images of the thin copper wire of the PSF phantom were acquired with a section thickness of 3 mm. The FWHM of the profiles for the various reconstruction kernels was 0.98 mm for UHR, 0.99 mm for HR, 1.13 mm for STD, 1.40 mm for SFT, and 1.86 mm for DS. A few checks with 1- and 5-mm sections gave the same results. From least-squares fits it was found that the PSFs for the DS, SFT, and STD kernel could reasonably well be described with a Gaussian, and those for the HR and UHR kernel only poorly. The results are used to calculate reconstruction filter and section thickness-dependent CT sample volumes.

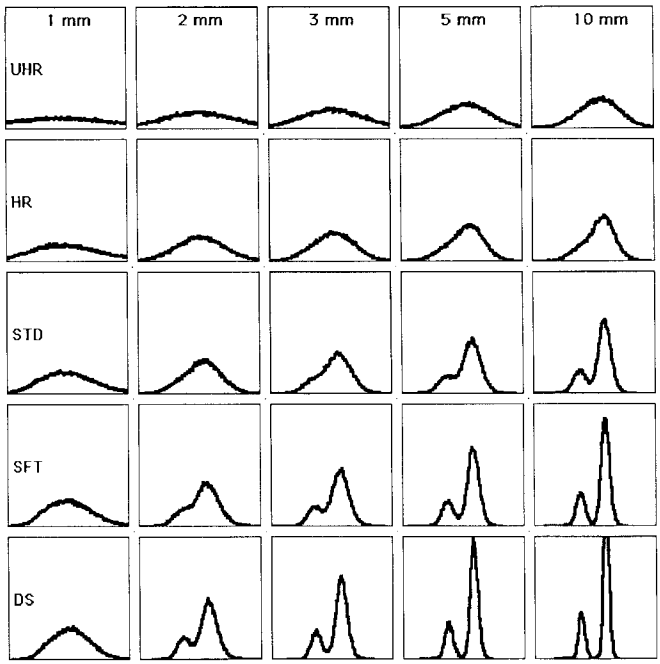

FIG. 1. Histograms from the PMMA thorax phantom containing foams of two densities, 63 and 96 kg/m^3, as a function of section thickness and reconstruction filter. Horizontal axis: CT number, range −1000 to −840 H, Vertical axis: pixel frequency, on identical vertical scales.

C. Histograms from PE foam and air: Density resolution and skewness

Density resolution for PE foam 109 measured free in air is shown in Fig. 3. For comparison, density resolution for air (in the images of foam 109) is shown in Fig. 4.

The average ratios of FWHM and s.d., obtained from the histograms from foams and air, are given in Table I.

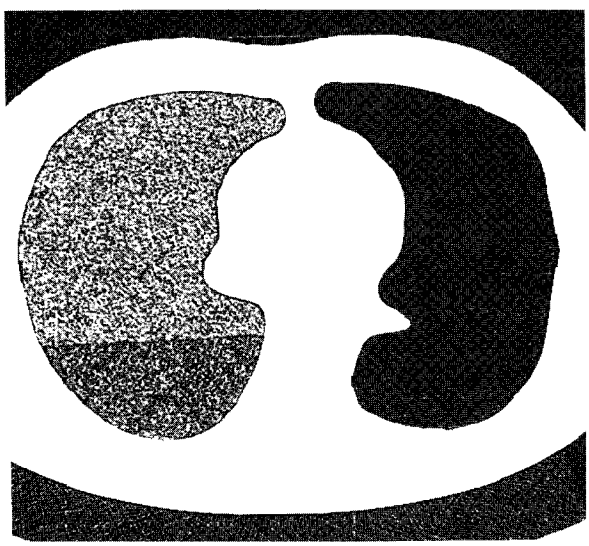

FIG. 2. PMMA thorax phantom with foams of two densities, 63 and 96 kg/m^3, covering 25% and 75% of the area of one lung cavity, the other cavity containing air. Image acquired with a section thickness of 1 mm and the UHR kernel.

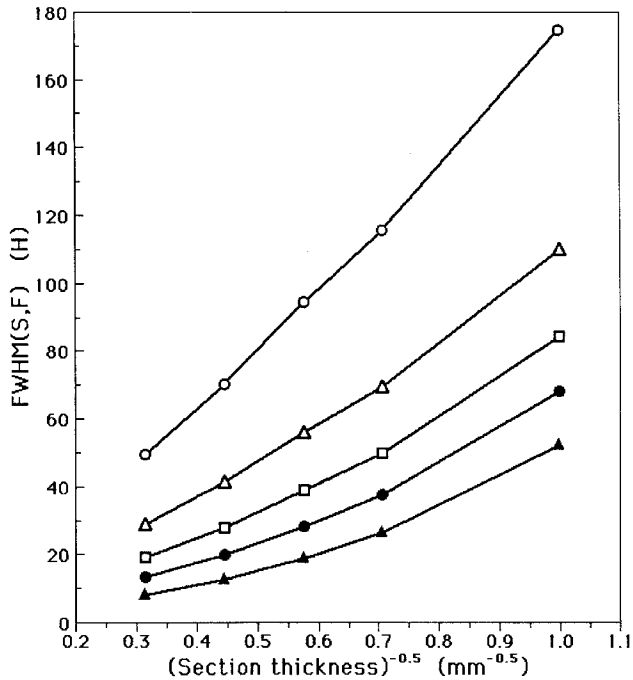

FIG. 3. Density resolution for foam 109 plotted as a function of the inverse square root of section thickness [see expression (8)]. From top to bottom: UHR, HR, STD, SFT, DS reconstruction filter.

The FWHMs of the histograms from the images whose matrix size had been reduced from the original 512×512 to 64×64 are also shown in Table I. The linear in-plane voxel size was 4.9 mm. The original image had been obtained with

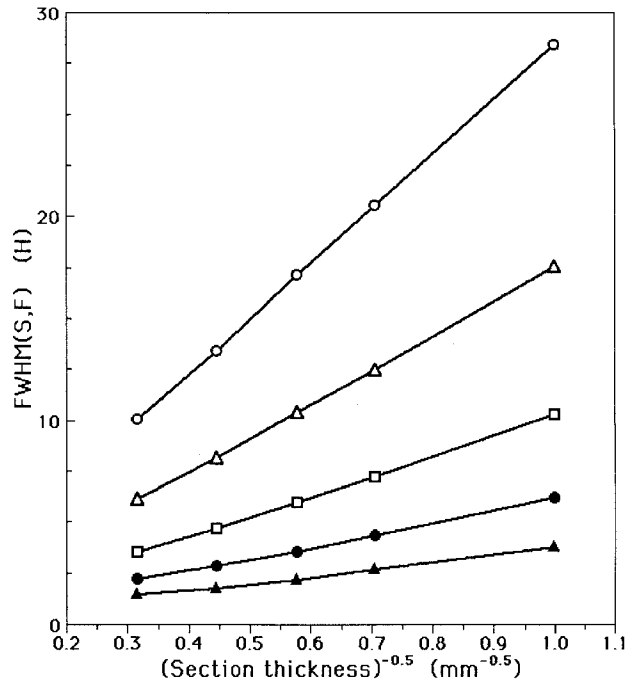

FIG. 4. Density resolution for air in scan of foam 109, plotted as a function of the inverse square root of section thickness. From top to bottom: UHR, HR, STD, SFT, DS reconstruction filter.

TABLE I. Foam histograms: FWHM for a 64×64 matrix, ratio FWHM/s.d. and average skewness.

	Foam					
	37	59	109	164	186	Air
$FWHM_{64\ matrix}$[a]	1.0 H	2.7 H	2.9 H	1.3 H	1.0 H	0.4 H
FWHM/sd[b]	2.18±0.13	1.98±0.14	2.05±0.08	2.02±0.14	2.36±0.05	2.30±0.11
Skewness[b]	0.43±0.16	0.76±0.23	0.57±0.18	0.55±0.14	−0.01±0.02	−0.03±0.04

[a]Voxel volume 240 mm^3 ($S=10$ mm, $L=4.9$ mm), averaged over 110 cm^2 of the foam image.
[b]Average over all combinations of section thickness and reconstruction kernel; normal 512×512 matrix.

a section thickness of 10 mm; the resulting sample volume was thus 240 mm^3. Small FWHMs of less than 3 H were obtained, reflecting good uniform average density as reported before.[1]

An example histogram from foam 109 is shown in Fig. 5. The histogram resembles a normal distribution, except for some positive skewness, as is illustrated by a fit of the left side, including the top, with a Gaussian. The skewness of the histograms from foam 109 is shown in Fig. 6. Values for the average skewness for foams and air are given in Table I.

D. Test of the hypothetic random cellular solid model [Expression (8)]

The decrease of the s.d. of the histograms with increasing section thickness was for all foams approximately according to the expected $S^{-1/2}$ dependence, at least when the points corresponding to a section thickness of 1 mm were excluded. Lines fitted to the data generally had small offsets, e.g., for foam 109 between −2.2 and −3.2 H. In all cases the offsets were relatively small compared to the measured s.d.'s.

Figure 7 shows the standard deviation of the histogram of foam 109 as a function of $V^{-1/2}$, with V the CT's sample volume. For the UHR and HR filter no appropriate estimates of sample volumes were available, as was discussed above; the corresponding reconstructions were not used in Fig. 7. Also, the measurements for 1-mm sections were not included. A good linear relationship, in agreement with expression (8), was observed. A similar behavior was found for all other foams. The offset and slope, obtained with linear regression analysis, are shown in Table II. From the values of the slopes it can be seen that density resolution for foam 37 was considerably better than for foam 109. For foams 59 and 164 it is similar to that for foam 109. Foam 186, which has very small cells of about 0.1 mm, had a density resolution nearly identical to that for air.

As a test of the dependence on foam characteristics, we calculated the ratio of the measured slope and the slope predicted by (8) using the foam characteristics given in Table II and $n=19$. This ratio should be a constant according to the model. The measured slope was first corrected for the contribution of quantum noise. Table II shows that the ratio is not really constant.

Varying the zoom factor used in reconstruction between 1 and 3 did not affect the CT number histograms, as judged from the average CT number and standard deviation.

E. Effect of quantum noise

In Fig. 8 the results from the study concerning the effect of quantum noise on density resolution are presented. For

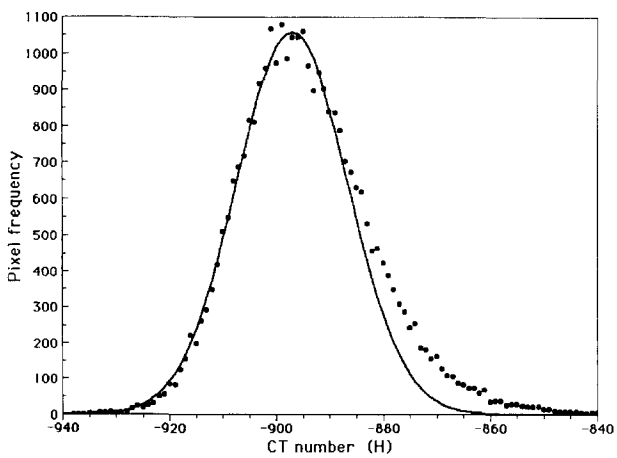

FIG. 5. Illustration of a histogram from foam 109 for a section thickness of 2 mm and the DS kernel (solid circles). Skewness was 0.66. Left side, including top, was fitted with a Gaussian (line) to show positive skewness of measured histogram.

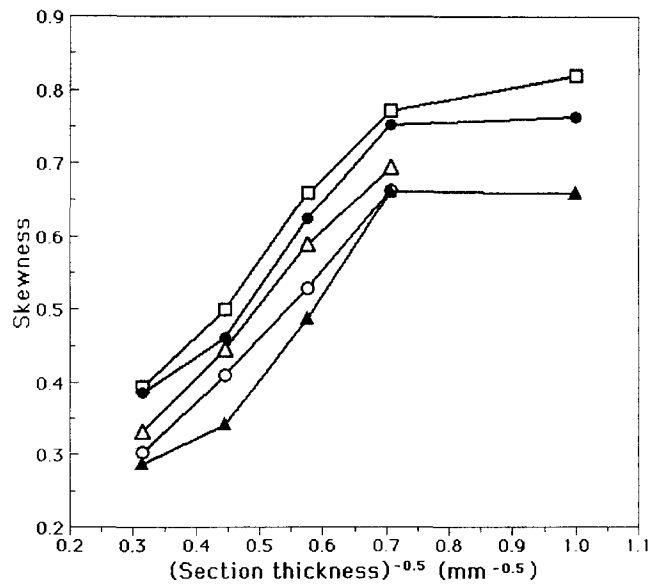

FIG. 6. Skewness of histograms from foam 109, arbitrarily plotted as a function of the inverse square root of section thickness, for kernels: UHR (open circle), HR (open triangle), STD (open square), SFT (closed circle), DS (closed triangle).

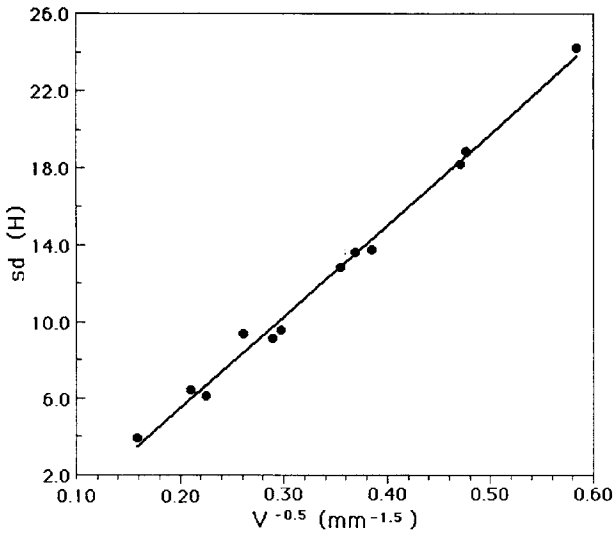

FIG. 7. Standard deviation of the histograms from foam 109 versus $V^{-1/2}$, with V the CT's sample volume, including a line fitted to the data. Data are for sections of 2, 3, 5, and 10 mm, each reconstructed with the DS, SFT, and STD reconstruction filters.

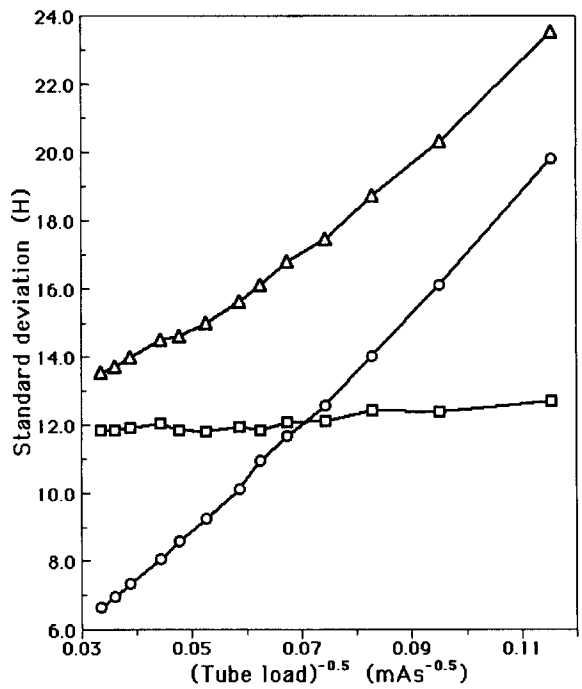

FIG. 8. Standard deviation of histograms from foam 37 (triangles) and air (circles) in the humanoid thorax phantom as a function of the inverse square root of mAs number. Also shown is the s.d. for the foam after elimination of the contribution of quantum noise (squares): $\text{s.d.}_{\text{corr}}=\sqrt{(\text{s.d.}^2_{\text{foam}}-\text{s.d.}^2_{\text{air}})}$.

foam 37 and air, both measured separately within the humanoid thorax phantom, the s.d.'s of the histograms are shown, together with the square root of the difference of their variances. The last parameter is nearly constant over the mAs range studied: 12.1±0.3 H.

F. Patients

The fit of expression (4) never failed, and convergence was always attained in a few iterations. The fit interval ranged from the lowest CT number in the histogram to about −650 H, but always included the whole peak at low density. An example of the input and output of the fit procedure is shown in Fig. 9. The values for $\text{FWHM}_{QN}(S,F)$ ("quantum noise"), needed in the fitting of (4), were obtained from the histograms of air in the empty lung cavity of the PMMA phantom (Table III). They were calculated as 2.35* s.d., rather than taking the directly measured FWHM values.

Data from patients A, B, and E could be fitted well with a power factor $\gamma=1$. For patient C the best results were obtained with $\gamma=1.5$ and for patient D with $\gamma=2$. For patient D a slightly lower $\gamma=1.5$ was in fact somewhat better for thin slices and sharp kernels, while $\gamma=2.5$ was more satisfactory for thick slices and smooth kernels. Also for the other patients small differences, the least for the sets that could be fitted with $\gamma=1$, were observed for the optimal γ. The rising slope of the fit at low CT numbers was reasonably sensitive to the estimate of $\text{FWHM}_{QN}(S,F)$. For curiosity, fitting data with a Gaussian whose width was independent of density ρ gave very poor results.

The results from the fits, $\text{FWHM}(S,\text{DS}\rightarrow F)$, were converted to $\text{FWHM}(S,F)$ using expressions (5) and (6). Values used for α_S [≡FWHM(S,DS)/FWHM(S,SFT)], determined as an average from foams 37, 59, 109, and 164, were $\alpha_{1\text{ mm}}=0.77\pm0.01$, $\alpha_{2\text{ mm}}=0.71\pm0.02$, $\alpha_{3\text{ mm}}=0.67\pm0.02$, $\alpha_{5\text{ mm}}=0.63\pm0.03$, and $\alpha_{10\text{ mm}}=0.62\pm0.02$. For patient A

TABLE II. Test of random cellular solid model.

	Foam					
	37	59	109	164	186	Air
Foam density ρ (kg/m^3)	37	59	109	164	186	1.2
Foam cell size D (mm)	1.5	1.5	1.0	0.8	0.1	···
Fit:						
Offset (H)	−0.8	−3.2	−4.1	−4.2	−0.3	−0.4
Slope (H/mm$^{3/2}$)	12.3	44.1	47.7	45.6	5.6	5.6
QN-corr slope[a] (H mm$^{3/2}$)	10.9	43.7	47.4	45.3	0.0	···
$\text{Slope}_{QN\text{-corr}}/\text{slope}_{\text{Eq. (8)}}$	0.7	1.8	1.9	1.7	0.0[b]	···

[a]For quantum noise corrected slope is $\sqrt{(\text{slope}^2_{\text{linfit foam}}-\text{slope}^2_{\text{linfit air}})}$.
[b]For foam 186 the calculated slope was 1.3 (H mm$^{3/2}$).

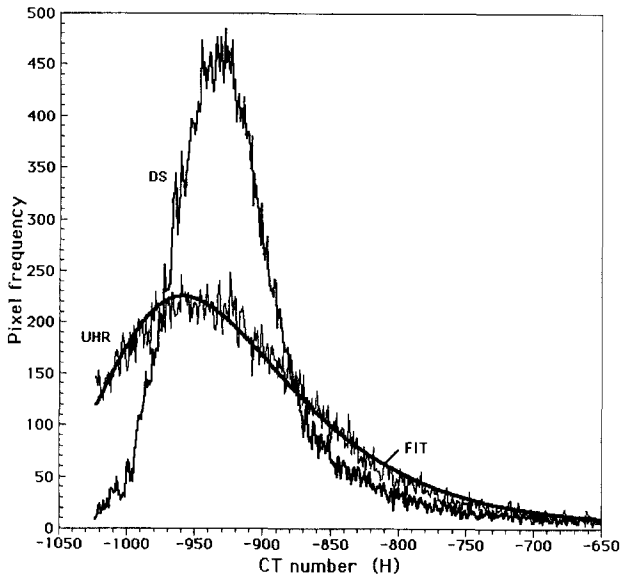

FIG. 9. Illustration of input (DS and UHR histograms) and output (FIT) of the fit procedure used in analyzing patient histograms (see text). Data are for patient A.

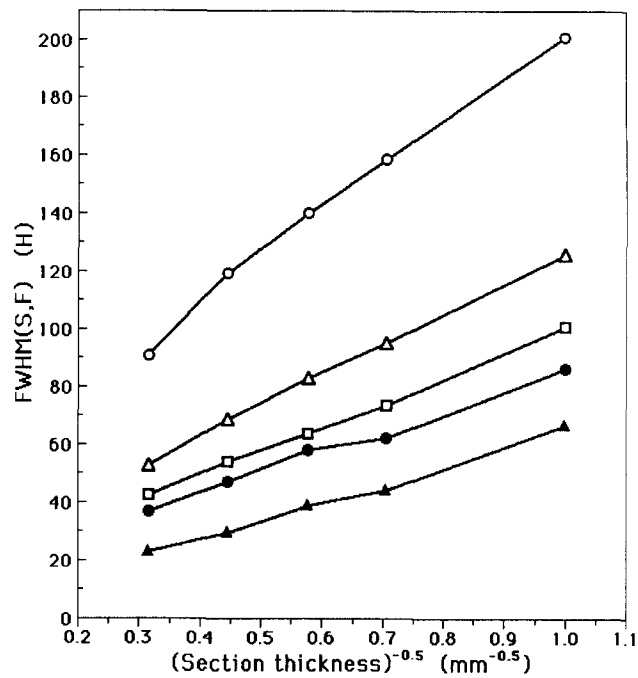

FIG. 10. Density resolution at average lung density (ρ_{av}=97 kg/m^3), FWHM(S,F), for patient A as a function of the inverse square root of section thickness. From top to bottom: UHR, HR, STD, SFT, DS reconstruction filter.

the results for FWHM(S,F) are shown in Fig. 10; for all other patients they are given in the Tables IV and V. Figure 10 and Table IV show all information of patients A and B, while Table V shows only the most relevant part of the data of patients C, D, and E.

A few illustrations of (the use of) the measured data are given. In Fig. 11 the density resolution FWHM(S,F,QN,ρ), according to expression (7), is shown for S=2 mm and F=DS, for all patients. The histogram of patient B, for a section thickness of 1 mm and the STD kernel, is shown in Fig. 12, together with a few Gaussians that show the density resolution at various CT numbers (−990, −950, −900, and −850 H). Figure 13 does the same, also for patient B, now for a section thickness of 2 mm and the DS kernel. The partially resolved peak at CT number −987 H corresponds to a series of bullae. Air in the main bronchi, not included in the region used in creating the histogram, had a CT number of −1007±6 H.

IV. DISCUSSION

A. Illustration of effect of density resolution

The importance of density resolution was, by way of introduction, illustrated in Fig. 1. Discrimination between the two densities of foam present in the PMMA thorax phantom is only possible for relatively smooth kernels and larger section thicknesses, notwithstanding the large difference in density of 33 kg/m^3. Contrary to what is the case in the histograms, the two foams can easily be discerned with the eye in all images corresponding to the histograms shown in Fig. 1. This may be verified in Fig. 2, where the image obtained with a section thickness of 1 mm and the UHR kernel is shown.

But does this example of poor density resolution have any bearing on patient studies? Yes, we think so. For instance, assuming lung with only the two densities the foams had, one can calculate a similar, "matrix" of histograms as in Fig. 1 using density resolution data from a patient. We performed these calculations with patient A's data and found even worse results than shown in Fig. 1.

From this phantom study it is concluded that visually observable contrast is not necessarily reflected in a histogram.

TABLE III. FWHM$_{QN}$(S,F) (H) of CT number histogram of air in PMMA thorax phantom.

Reconstruction filter F	Section thickness S (mm)				
	1	2	3	5	10
UHR	78.7	55.6	53.5	44.7	38.6
HR	53.9	41.9	36.0	29.4	24.5
STD	36.5	27.8	24.3	19.5	15.1
SFT	25.2	18.6	16.0	13.0	10.1
DS	17.0	12.7	10.8	8.9	7.3

TABLE IV. Density resolution FWHM(S,F) (H) for patient B (emphysema, 63 y,m).[a]

Reconstruction filter F	Section thickness S (mm)				
	1	2	3	5	10
UHR	189	136	124	106	79
HR	108	80	74	66	47
STD	79	57	55	53	35
SFT	50	37	35	31	19
DS	39	26	23	20	12

[a]Power factor γ in expressions (1)–(7) is 1.0; ρ_{av}=107 kg/m^3.

TABLE V. Density resolution FWHM(S,F) (H) for patients C, D, and E.

Patient	Recon. filter F	Section thickness S (mm) 1	2	3	5	10
C[a]	STD	119	85	75	58	42
	SFT	89	65	60	45	31
	DS	68	46	40	28	19
D[b]	STD	99	61	54	47	39
	SFT	78	51	45	39	31
	DS	60	36	30	25	20
E[c]	STD	147	128	116	100	86
	SFT	124	99	89	79	67
	DS	96	70	60	50	41

[a]Emphysema, 79 y,m; γ in expressions (1)–(7) is 1.5; $\rho_{av}=142$ kg/m^3.
[b]Normal lungs, 69 y,m; $\gamma=2.0$; $\rho_{av}=139$ kg/m^3.
[c]Emphysema and interstitial disease, 83 y,m; $\gamma=1.0$; $\rho_{av}=215$ kg/m^3.

Therefore, in designing any form of density "spectroscopy," quantitative data on density resolution should preferably be used.

B. Spatial resolution and CT sample volume

Density resolution is strongly dependent on section thickness and reconstruction kernel, as was shown in Fig. 1. Given the scanner's hardware, these parameters are also the determinants of spatial resolution, or equivalently, the volume in the scanned object over which the signal is averaged before it is shown in a pixel of the image. In the direction perpendicular to the scan plane the sample dimension is equal to the section thickness (S). The in-plane dimensions are normally determined by the reconstruction kernel. Kernels that result in a (nearly) Gaussian point spread function (PSF) can be characterized completely by a single width parameter, e.g., the standard deviation σ[28], and the corresponding effective in-plane sample width is $L=(2\pi)^{1/2}/\sigma=2.51\sigma$, which is nearly equal to the FWHM (2.35σ). Gaussian PSFs were found for the DS, SFT, and STD kernels, in agreement with what was reported in the literature.[28]

To give an example of the use of the present data, making a scan with a 2-mm section thickness and the smoothest (DS)

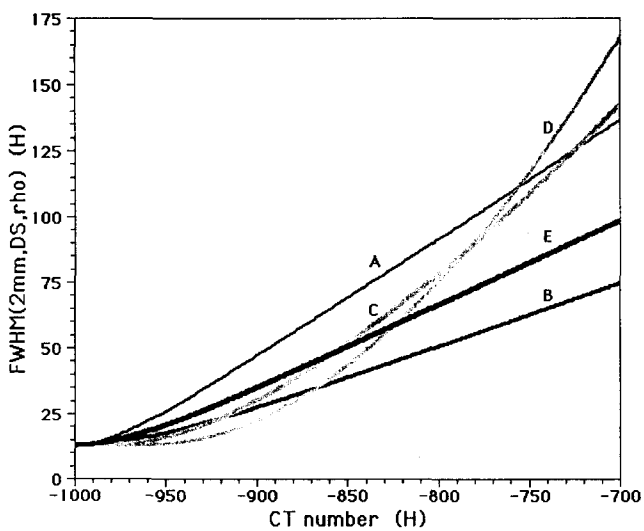

FIG. 11. Density resolution for patients A–E as a function of CT number. Section thickness 2 mm and DS reconstruction filter. Curves are labeled with patient number.

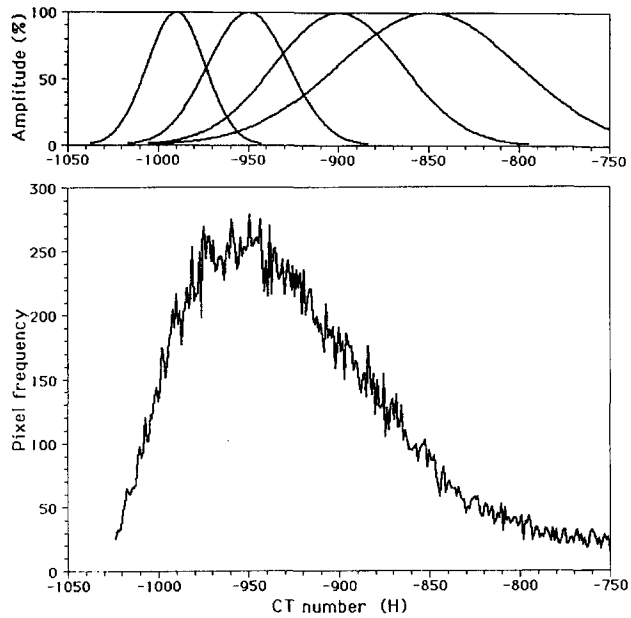

FIG. 12. Bottom: Histogram of patient B for a section thickness of 1 mm and the STD reconstruction filter. Top: Illustration of density resolution at various CT numbers. Note for instance that densities corresponding to a CT number of −900 H, or even −850 H, must have been "misplaced" to a considerable fraction in the histogram below −950 H.

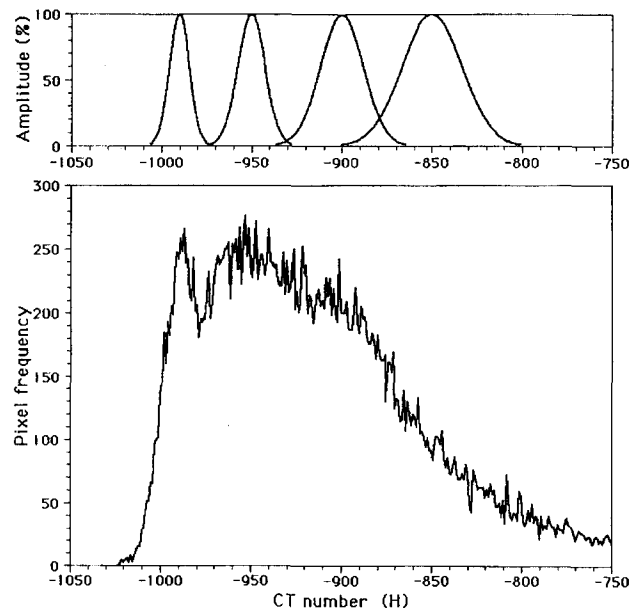

FIG. 13. Bottom: Histogram of patient B for a section thickness of 2 mm and the DS reconstruction filter. Note the partially resolved peak at −987 H corresponding to lung bullae. Top: Illustration of density resolution at various CT numbers.

kernel results in a sample volume of approximately $V=SL^2=2\times1.99^2=8$ mm^3. High resolution kernels, having negative side lobes in their PSF, can no longer fully be characterized by a single width parameter, and the definition of sample volume is more difficult and was not tried.

C. PE foams

The reason for studying foams was the expectation that it would help in understanding the properties of lung tissue in CT densitometry. The foams used have the advantage over lung tissue in that they are uniform, at least at a scale above that of individual cells. This uniformity was proven by the small FWHM of the histograms when the foams were measured with a large sample volume of about 240 mm^3 (Table I). As already explained, uniformity is a prerequisite for the direct estimation of density resolution from the width of a measured histogram.

Density resolution for the coarser foams, of 37, 59, 109, and 164 kg/m^3, was generally much worse than for air. Foam 186, on the other hand, having cells considerably smaller than even the smallest sample volume, gave a density resolution that was similar to that for air. For air density resolution is determined by quantum noise or, to be more precise, by system noise, which also includes small contributions from instrumental noise. For foam an additional component, the effect of sampling a cellular solid, exists, and this component clearly dominates density resolution for the coarser foams. On physical grounds one expects these two components, i.e., quantum noise and sampling effects, to be independent, as was assumed in writing expression (4). If this is the case the density resolution for foam should be independent of mAs after elimination of the contribution of quantum noise. According to our study of foam 37 and air in the humanoid thorax phantom this is indeed the case (Fig. 8).

All foam histograms, except those from the fine-cellular foam 186, were slightly skewed towards higher CT numbers. They resemble, in fact, Poisson distributions with a low average value, and this might essentially be the case.

A point of some interest is the functional dependence of density resolution on the CT's sample volume and the foam's density and cell size. Unfortunately, we only have a rather crude model, leading to expression (8). A first test of the model was the dependence of density resolution on the inverse of the square root of section thickness. An acceptable linear dependence between the two quantities was generally observed (see, e.g., Fig. 3), at least when the data for the sections of 1 mm were discarded. This latter seems not unreasonable, since all foams have cell sizes of the order of 1 mm, while the model only may be expected to work when the sample volume is sufficiently larger than the cell volume. The dependence of density resolution on sample volume V conforms to expression (8), at least for sections thicker than 1 mm and kernels that have a Gaussian PSF (Fig. 7). As a final test of the model we calculated the ratio of measured and predicted slope of the s.d. versus the $V^{-1/2}$ curve. This ratio should be a constant, independent of foam type. The results presented in the bottom row of Table II show that this is only roughly the case. In summary, it appears that expression (8), notwithstanding the shortcomings of the underlying physical model, gives an adequate description of the dependence of density resolution on CT technique parameters (S and V), and a rather poor description of the dependence on foam characteristics (ρ and D).

D. Patients

CT number histograms of lung tissue usually have no features that allow the immediate determination of the density resolution that was available while generating the image. Therefore, to obtain quantitative data on density resolution for lung, some indirect method had to be applied. We have chosen as the first step for determining the reconstruction, kernel-dependent degradation of density resolution relative to the DS reconstruction of the scan of the same section thickness. The second step consisted in converting the differences in density resolution so obtained into absolute values, using information gathered from the foams. Only the low density range, typically below -650 H, was analyzed in all studies. The high density tail in the histograms, generally accounting for less than 5% of the area of the lung, was not included in the analysis.

The degradation in density resolution caused by sharper kernels was determined with a robust combination of a convolution algorithm and a nonlinear least-squares fit procedure. In the fit the density resolution was assumed to be density dependent. For simplicity we assumed that the dependence could be modeled by some power γ of the density. Optimization of this power factor γ yielded for three patients $\gamma=1$ and for the remaining two $\gamma=1.5$ and $\gamma=2.0$, respectively. However, some caution with respect to the magnitude of γ is in order, as we learned in our experience with foams. In all measurements on the coarser foams slightly skewed histograms were observed. Transforming a DS histogram of foam into one for a sharper kernel required a similarly skewed distribution. This was verified by performing a number of deconvolutions using the FFT method. But convolution with a Gaussian always reduces skewness, and it will be remembered that we used a Gaussian in the analysis of the patient studies. Therefore, applying the same method to the foams as used for the patients, but with the density dependence removed because the foams are of uniform density, resulted in poor fits of too low skewness. Good fit quality could be restored by introducing the (now unphysical) ρ dependence, because this very effectively simulated convolution with a skewed function, as is easily understood: points to the right in the DS histogram are redistributed over a wider range than points to the left, according to expression (4). Since it is likely that the correct convolution function for lung tissue has also positive skewness, these observations lead to the conclusion that the experimental values for γ are probably upper limits. The random cellular solid model predicts $\gamma=1$ when there is no relation between characteristic structural dimensions and density, but whether this is the case is unknown.

In the calculation of absolute estimates of density resolu-

tion we used α_s values, i.e., ratios of density resolution for the DS and SFT kernel, derived from foam studies. These ratios were nearly independent of foam type, and not too different from those for air. It seems reasonable to expect similar values for lung. To give an idea of the sensitivity to this parameter, a change of 10% in α_s caused a change of about 20% in the estimate of density resolution for the DS kernel. The effect on density resolution for the other kernels is much less, because the first term under the square root in expression (6) usually dominates the second, the latter being the only one affected by α_s.

A further point of concern might be correlation between noise in the images. In the quantitative analysis we appeared to assume that the noise contribution in the image reconstructed with kernel F was independent from the noise in the DS image. Since we used images that were reconstructed from the same scan data this will not be the case, even when the kernels are different. However, we analyzed histograms from the images, and these are hardly sensitive to the actual noise pattern: Measuring air or foam several times gave the same results in terms of overall histogram shape, as characterized by the standard deviation. Making independent scans, instead of using one as we did, would therefore have given virtually the same histograms. Correlation effects should therefore be negligible, especially since we essentially used the global shape of the histograms in our analysis.

Between patients' differences in density resolution clearly exist, although the differences are generally smaller than a factor of 2, both at the average density of the lung studied (Fig. 10 and Tables IV and V) and at corresponding densities (Fig. 11). In Fig. 11 the curve for patient D with $\gamma=2$ deviates somewhat more but, as already discussed, the high power factor may be unrealistic.

The important question now is: how realistic are our estimates of density resolution for lung tissue? Regarding the approximate average density resolution, we think our estimates are realistic, simply because a certain amount of broadening has to be accounted for and this requires values of the order of magnitude given. As to the functional dependence of density resolution on ρ, we can make no definite statements except that the sampling component in density resolution should go to zero together with ρ. Consequently, quantum noise will determine density resolution at low density.

Coming to the practical implications of our results, several aspects appear of importance. Regarding the use of histogram related parameters other than the average density, it must be expected that large but varying changes are introduced by changing section thickness and reconstruction kernel. The actual change in each individual case will depend on the (beforehand unknown) distribution of densities in the lung that is smeared out by the finite density resolution. It seems possible that poor density resolution enhances correlation between average density and other histogram related parameters. The only way to guarantee meaningful numbers under all circumstances is to use sufficient density resolution.

Several investigators,[14–16,18–21] including the authors,[12] used thin sections (1 mm) in combination with standard or high resolution reconstruction kernels. For high resolution CT (HRCT), used for the visual assessment of lung disease, this technique has shown its potential.[29–31] For densitometry the situation is quite different, however. The present results indicate that the ensuing density resolution is generally quite bad. This is illustrated in Fig. 12 for the STD filter. The Gaussians show the poor resolution at various CT numbers. Notice also that the histogram is without any features (apart from noise). The same conclusion can be drawn from the corresponding histogram in Fig. 1, as this figure is also reasonably representative for lung of corresponding densities. For the HR filter density resolution is still considerably worse. In our opinion this so-called thin section technique is not appropriate for density "spectroscopy," except in determining average density.[1,2] Another way of looking at this point of small sample volumes is to realize that density is only a meaningful parameter when it is obtained from a volume larger than the characteristic structural dimensions. From the similarity between lung and the coarse foams, it appears that the relevant dimensions in lung are of the order of magnitude of 1 mm and that CT samples should be larger than this.

Other investigators[3–11,13–15,17] have used section thicknesses larger than 1 mm, but to our knowledge always in combination with standard or high resolution kernels. For our scanner the effective in-plane sample width is approximately 1.2 mm for the STD kernel, and for other scanners it is probably similar. The combination of thick sections and a smaller in-plane sample size appears not appropriate from a sampling point of view, because density is averaged over rodlike volumes where lesions probably do not favor this shape. More or less spherical or cubic samples probably warrant less undesired density averaging. Since the volume of a sphere or a cube changes with the third power of the linear dimension, small changes already have a large impact. Probably no suitable reconstruction kernels are currently available to increase in-plane sample width to above 2 mm. Reducing matrix size, or using image filtering, might be employed as alternatives if required.

Finally, the optimal compromise between spatial and density resolution may depend on the kind of the lesions and the difference in density between affected and unaffected tissue, and might be the subject of future research.

V. CONCLUSIONS

The importance of density resolution, a parameter so far totally neglected in densitometry of the lungs, was illustrated.

For a number of foams that served as simple models of lung, density resolution was determined as the FWHM of the CT number histogram. Density resolution for foams with cells of 0.8–1.5 mm was dominated by sampling effects in these cellular solids, and was very poor for thin sections and sharp reconstruction filters. The contribution of quantum noise was generally small. The zoom factor used in reconstruction did not affect density resolution on this scanner.

Variations in density resolution for the different foams studied could roughly be explained by a simple model derived for a hypothetical random cellular solid.

A phenomenological description for density-dependent density resolution for lung tissue was presented. An experimental method, using this description in a combined convolution least-squares fit procedure, was developed and applied to determine section thickness and reconstruction kernel-dependent density resolution in patient studies. Uncertainty remains concerning the functional dependence of density resolution on structure related lung characteristics.

Also, in patient studies density resolution was quite poor for thin sections and/or sharp kernels. The results indicate that parameters that depend on the shape of the histogram will be rather sensitive to density resolution. Only in the presence of sufficient density resolution will meaningful values be obtained. Thin section densitometry, i.e., using 1-mm sections in combination with a standard or high resolution reconstruction kernel, should not be used except in determining average density. When using thicker sections, it is advised to use an in-plane spatial resolution that is similar to section thickness, contrary to what has been general practice so far.

ACKNOWLEDGMENTS

We would like to thank Dr. J. Timmer, Scanner Science CT, Philips Medical Systems, Best, for his comment on the manuscript, G.G.H. Wijnhoven from our hospital for his support of our CT densitometry research, and Dr. M.A.O. Thijssen, University Hospital Nijmegen, for putting the humanoid thorax phantom at our disposal.

[1]G. J. Kemerink, R. J. S. Lamers, G. R. P. Thelissen, and J. M. A. van Engelshoven, "CT-densitometry of the lungs: scanner performance," J. Comput. Assist. Tomogr. **20**, 24–33 (1996).

[2]G. J. Kemerink, R. J. S. Lamers, G. R. P. Thelissen, and J. M. A. van Engelshoven, "Scanner conformity in CT densitometry of the lungs," Radiology **197**, 749–752 (1995).

[3]M. D. Hayhurst, D. C. Flenley, A. McLean, A. J. A. Wightman, W. MacNee, D. Wright, D. Lamb, and J. Best, "Diagnosis of pulmonary emphysema by computerized tomography," The Lancet **11**, 320–323 (1984).

[4]N. L. Müller, C. A. Staples, R. R. Miller, and R. T. Abboud, " "Density Mask": An objective method to quantitate emphysema using computed tomography," Chest **94**, 782–787 (1988).

[5]G. A. Gould, W. Macnee, A. McLean, P. M. Warren, A. Redpath, J. J. K. Best, D. Lamb, and D. C. Flenley, "CT measurements of lung density in life can quantitate distal airspace enlargement: An essential defining feature of human emphysema", Am. Rev. Respir. Dis. **137**, 380–392 (1988).

[6]B. H. Fromson and D. M. Denison, "Quantitative features in the computed tomography of healthy lungs," Thorax **43**, 120–126 (1988).

[7]Y. Kitahara, M. Takamoto, M. Manuyama, Y. Tanaka, T. Ishibashi, and A. Shinoda, "Differential diagnosis of pulmonary emphysema using the CT index: LL%w," Nippon Kyobu Shikkan Gakkai Zasshi **27**, 689–695 (1989).

[8]M. Kinsella, N. L. Müller, R. T. Abboud, N. J. Morrison, and A. Dybuncio, "Quantitation of emphysema by computed tomography using a "Density Mask" program and correlation with pulmonary function tests," Chest **97**, 315–321 (1990).

[9]R. J. Knudson, J. R. Standen, W. T. Kaltenborn, D. E. Knudson, K. Rehm, M. P. Habib, and J. D. Newell, "Expiratory computed tomography for assessment of suspected pulmonary emphysema," Chest **99**, 1357–1366 (1991).

[10]H. Adams, M. S. Bernard, and K. McConnochie, "An appraisal of CT pulmonary density mapping in normal subjects," Clin. Radiol. **43**, 238–242 (1991).

[11]D. C. Archer, C. L. Coblentz, R. A. deKemp, C. Nahmias, and G. Norman, "Automated *in vivo* quantification of emphysema," Radiology **188**, 835–838 (1993).

[12]R. J. Lamers, G. R. Thelissen, A. G. Kessels, E. F. Wouters, and J. M. van Engelshoven, "Chronic obstructive pulmonary disease: Evaluation with spirometrically controlled CT lung densitometry," Radiology **193**, 109–113 (1994).

[13]W. Biernacki, G. A. Gould, K. F. Whyte, and D. C. Flenley, "Pulmonary hemodynamics, gas exchange, and the severity of emphysema as assessed by quantitative CT scan in chronic bronchitis and emphysema," Am. Rev. Respir. Dis. **139**, 1509–1515 (1989).

[14]W. A. Kalender, R. Rienmüller, W. Seissler, J. Behr, M. Welke, and H. Fichte, "Measurement of pulmonary parenchymal attenuation: Use of spirometric gating with quantitative CT," Radiology **175**, 265–268 (1990).

[15]W. A. Kalender, H. Fichte, W. Bautz, and M. Skalej, "Semiautomatic evaluation procedures for quantitative CT of the lung," J. Comput. Assist. Tomogr. **15**, 248–255 (1991).

[16]R. K. Rienmüller, J. Behr, W. A. Kalender, M. Schätzl, I. Altmann, M. Merin, and T. Beinert, "Standardized quantitative high resolution CT in lung diseases," J. Comput. Assist. Tomogr. **15**, 742–749 (1991).

[17]G. A. Gould, A. T. Redpath, M. Ryan, P. M. Warren, J. J. K. Best, E. J. W. Cameron, and W. MacNee, "Parenchymal emphysema measured by CT lung density correlates with lung function in patients with bullous disease," Eur. Respir. J. **6**, 698–704 (1993).

[18]R. Rienmüller, M. Schätzl, W. Kalender, F. Krombach, and E. Fiehl, "Quantitative CT-Untersuchungen der Lunge am tierexperimentellen Modell der Silikose," Fortschr. Röntgenstr. **148**, 367–373 (1988).

[19]P. Kohz, A. Stäbler, T. Beinert, J. Behr, T. Egge, A. Heuck, and M. F. Reiser, "Reproducibility of quantitative, spirometrically controlled CT," Radiology **197**, 339–342 (1995).

[20]T. Beinert, J. Behr, F. Mehnert, P. Kohz, M. Seemann, R. Rienmüller, and M. Reiser, "Spirometrically controlled quantitative CT for assessing diffuse parenchymal lung disease," J. Comput. Assist. Tomogr. **19**, 924–931 (1995).

[21]P. G. Hartley, J. R. Galvin, G. W. Hunninghake, J. A. Merchant, S. J. Yagla, S. B. Speakman, and D. A. Schwartz, "High-resolution CT-derived measures of lung density are valid indexes of interstitial lung disease," J. Appl. Physiol. **76**, 271–277 (1994).

[22]ICRU Report No. 44. "Photon, electron, proton and neutron interaction data for body tissues," International Commission on Radiation Units and Measurements, 7910 Woodmont Avenue, Bethesda, MD 20814 (1989).

[23]T. S. Curry, J. E. Dowdey, and R. C. Murry, *Christensen's Physics of Diagnostic Radiology* (Lea & Febiger, Philadelphia, 1990), p. 316.

[24]J. G. Pearce, E. N. C. Milne, G. D. Gillan, and W. W. Roeck, "Development of a radiographic chest phantom with disease simulation," Invest. Radiol. **14**, 181–184 (1979).

[25]G. J. Kemerink, R. J. S. Lamers, G. R. P. Thelissen, and J. M. A. van Engelshoven, "The nonlinear partial volume effect and computed tomography densitometry of foam and lung," Med. Phys. **22**, 1445–1450 (1995).

[26]P. R. Bevington, *Data reduction and error analysis for the physical sciences* (McGraw-Hill Book Company, New York, 1969).

[27]L. J. Gibson and M. F. Ashby, *Cellular Solids: Structure and Properties* (Pergamon, Oxford, 1988).

[28]E. L. Nickoloff and R. Riley, "A simplified approach for modulation transfer function determinations in computed tomography," Med. Phys. **12**, 437–442 (1985).

[29]R. H. Hruban, M. A. Meziane, E. A. Zerhouni, N. F. Khouri, E. K. Fishman, P. S. Wheeler, J. S. Dumler, and G. M. Hutchins, "High resolution computed tomography of inflation-fixed lungs," Am. Rev. Resp. Dis. **136**, 935–940 (1987).

[30]R. R. Miller, N. L. Müller, S. Vedal, N. J. Morrison, and C.A. Staples, "Limitations of computed tomography in the assessment of emphysema," Am. Rev. Resp. Dis. **139**, 980–983 (1989).

[31]K.-Kuwano, K. Matsuba, T. Ikeda, J. Murakami, A. Araki, H. Nishitani, T. Ishida, K. Yasumoto, and N. Shigematsu, "The diagnosis of mild emphysema: Correlation of computed tomography and pathology scores," Am. Rev. Resp. Dis. **141**, 169–178 (1990).